Received: 26 April 2021 | Revised: 28 May 2021 | Accepted: 7 June 2021

DOI: 10.1002/pol.20210304

RESEARCH ARTICLE

JOURNAL OF POLYMER SCIENCE WILEY

Reformulating the permselectivity-conductivity tradeoff relation in ion-exchange membranes

Jovan Kamcev

Department of Chemical Engineering, Macromolecular Science and Engineering, University of Michigan, North Campus Research Complex, Ann Arbor, Michigan, USA

Correspondence
Jovan Kamcev, Department of Chemical Engineering, Macromolecular Science and Engineering, University of Michigan, North Campus Research Complex, B28, 2800 Plymouth Rd., Ann Arbor, MI 48109, USA.
Email: jkamcev@umich.edu

Abstract

Polymer membranes used in separation applications exhibit a tradeoff between permeability and selectivity. That is, membranes that are highly permeable tend to have low selectivity and vice versa. For ion-exchange membranes used in applications such as electrodialysis and reverse electrodialysis, this tradeoff is expressed in terms of membrane permselectivity (i.e., ability to selectively permeate counter-ions over co-ions) and ionic conductivity (i.e., ability to transport ions in the presence of an electric field). The use of membrane permselectivity and ionic conductivity to illustrate a tradeoff between counter-ion throughput and counter-ion/co-ion selectivity in ion-exchange membranes complicates the analysis since permselectivity depends on the properties of the external solution and ionic conductivity depends on the transport of all mobile ions within a membrane. Furthermore, the use of these parameters restricts the analysis to ion-exchange membranes used in applications in which counter-ion/co-ion selectivity is required. In this study, the permselectivity-conductivity tradeoff relation for ion-exchange membranes is reformulated in terms of ion concentrations and diffusion coefficients in the membrane. The reformulated framework enables a direct comparison between counter-ion throughput and counter-ion/co-ion selectivity and is general. The generalizability of the reformulated tradeoff relation is demonstrated for cation-exchange membranes used in vanadium redox flow batteries.

KEYWORDS

electrodialysis, ion-exchange membranes, ionic conductivity, permselectivity, vanadium redox flow batteries

1 | INTRODUCTION

Dense polymer membranes with ionizable functional groups covalently bound to their backbone (i.e., ion exchange membranes [IEMs]) are key components of several separation technologies (e.g., electrodialysis,[1,2] chemical synthesis,[3,4] diffusion dialysis[5]) and energy generation technologies (e.g., reverse electrodialysis,[6,7] fuel cells[8,9]). IEMs also play a key role in emerging environmental and energy applications such as redox flow batteries,[10,11] microbial fuel cells,[12] ion-exchange membrane bioreactors,[13] and electrochemical CO_2 reduction,[14,15] among others. Membranes with tailored selectivity and improved throughput are needed to increase the efficiency of existing technologies and to enable the use of IEMs in new applications. However, research efforts over the past several decades have resulted in only marginal improvements in membrane performance, largely due to poorly understood material limitations and incomplete fundamental knowledge of transport phenomena in such materials.

IEMs are used to mediate the transport of various ionic and neutral solutes. In general, IEMs are required to efficiently permeate counter-ions (i.e., ions with a charge opposite to that of the fixed charge groups) while preventing the passage of other solutes. For example, IEMs used in electrodialysis (ED) and reverse electrodialysis (RED) must prevent the transport of co-ions (ions with a similar charge to that of the fixed charge groups) and water.[16] The ability of IEMs to preferentially permeate counter-ions over co-ions is generally quantified by the membrane permselectivity.[17] In the presence of an electric field, ion transport across IEMs is quantified by the membrane ionic conductivity.[17] High-performance membranes for ED/RED should have both high ionic conductivity and high permselectivity. However, currently available IEMs are bound by a tradeoff between membrane permselectivity and ionic conductivity.[18] That is, membranes that have high ionic conductivity generally have low permselectivity and vice versa. A similar tradeoff between membrane throughput and selectivity is observed for virtually all synthetic polymer membranes, regardless of the application.[19] Figure 1 illustrates the tradeoff between apparent permselectivity and ionic conductivity for various cation and anion exchange membranes (CEMs and AEMs). Permselectivity-conductivity plots are commonly used to evaluate the performance of new IEMs relative to that of existing materials.[20–26]

Permselectivity is not an intrinsic membrane property since it depends on the properties of the solution contacting the membrane. Moreover, ionic conductivity depends on the transport of both counter-ions and co-ions, so high ionic conductivity does not necessarily mean that the electrical current is carried entirely by the counter-ions, which is the optimal scenario for applications that use IEMs. Taken together, these complications make it difficult to conclude that the observed tradeoff behavior is due to intrinsic membrane properties. Further, the use of membrane permselectivity restricts the analysis to IEMs that are used for applications such as ED/RED, in which counter-ion/co-ion selectivity is important. The analysis does not apply directly to IEMs used in applications in which selectivity between different counter-ions is important (e.g., diffusion dialysis, flow batteries, etc.). In this study, the permselectivity-conductivity tradeoff relation for IEMs is reformulated in terms of ion concentrations and diffusion coefficients in the membrane, which are fundamental membrane parameters that characterize individual ion transport in the membrane. The reformulated tradeoff relation is general and consistent with the permeability-selectivity tradeoff relation discussed in the gas separation and reverse osmosis bodies of literature.

2 | BACKGROUND

The ability of IEMs to permeate counter-ions over co-ions is generally quantified by the membrane permselectivity, Π, which is defined as[17]:

$$\Pi = \frac{t_g^m - t_g^s}{t_c^s} = \frac{t_g^m - t_g^s}{1 - t_g^s} \tag{1}$$

where t_g^m and t_g^s are the counter-ion transport numbers in the membrane and external solution, respectively, and t_c^s is the co-ion transport number in the external solution. The transport number of ion i in phase j, t_i^j, is defined as the fraction of current that is carried by ion i in the presence of an electric field, or:

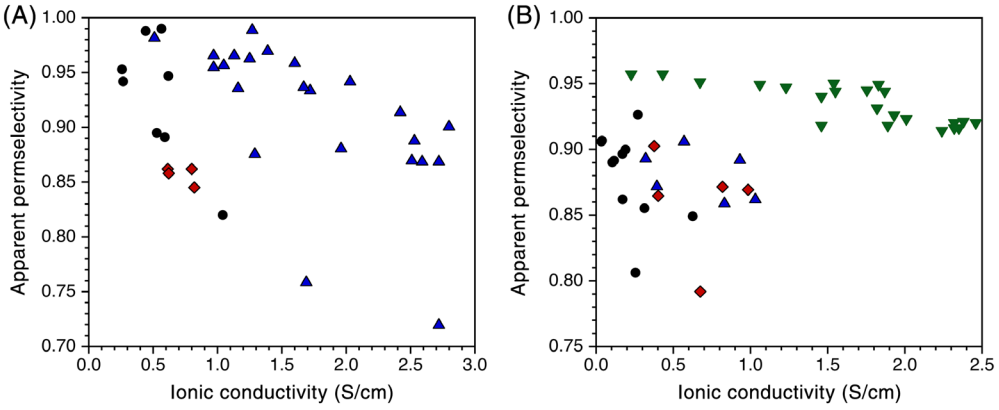

FIGURE 1 Correlation between apparent permselectivity and ionic conductivity for various (A) CEMs and (B) AEMs. The different symbols represent results from different studies. The data used to generate these plots are tabulated in Data S1. In all cases, ionic conductivity measurements were performed using membranes equilibrated with 0.5 M NaCl solutions and apparent permselectivity values were calculated from membrane potential measurements performed with 0.1 M NaCl solution on one side of the membrane and 0.5 M NaCl solution on the other side of the membrane

$$t_i^j = \frac{z_i F J_i^j}{I} = \frac{z_i J_i^j}{\sum_i z_i J_i^j} \tag{2}$$

where z_i is the valence of ion i, J_i^j is the flux of ion i in phase j, F is Faraday's constant, and I is the current density. The one-dimensional Nernst-Planck equation provides an expression for J_i^j:

$$J_i^j = -D_i^j \frac{dC_i^j}{dx} - z_i F C_i^j u_i^j \frac{d\psi^j}{dx} \tag{3}$$

where C_i^j, D_i^j, and u_i^j are the concentration, diffusivity, and absolute mobility of ion i in phase j, respectively, ψ^j is the electric potential of phase j, and x is the direction of transport (generally across the membrane thickness). This form of the Nernst-Planck equation assumes that ion activity coefficients in the membrane do not change along the membrane thickness and neglects convective ion transport, which are reasonable assumptions for conventional IEMs.[27] Inserting Equation 3 into Equation 2 and neglecting the concentration-gradient term yields an expression for the transport number in terms of ion concentrations and absolute mobilities (or diffusivities)[27,28]:

$$t_i^j = \frac{z_i^2 C_i^j u_i^j}{\sum_i z_i^2 C_i^j u_i^j} = \frac{z_i^2 C_i^j D_i^j}{\sum_i z_i^2 C_i^j D_i^j} \tag{4}$$

On the right-most side of Equation 4, ionic absolute mobilities were related to ionic diffusivities using the Einstein equation ($u_i = D_i/(RT)$, where R is the gas constant and T is absolute temperature). The Einstein equation is strictly valid for infinitely dilute systems in which coupling of ionic fluxes is negligible, but this relationship appears to hold reasonably well for conventional IEMs.[27] For a perfectly selective membrane, $t_g^m = 1$ and $\Pi = 1$. As Π approaches zero, t_g^m approaches t_g^s, and the membrane imparts no counter-ion transport selectivity relative to an aqueous solution. Equations 1–4 demonstrate that permselectivity is not an intrinsic membrane property. Permselectivity depends on both the nature of the ions as well as the concentration and mobility of the ions in the contiguous solution.

Membrane permselectivity measurements are generally performed using the so-called static method, which involves placing a membrane between two aqueous salt solutions having different concentrations and measuring the electric potential difference across the membrane (i.e., the membrane potential).[17] The membrane potential, ψ_m, which consists of the Donnan potential at each membrane-solution interface and the diffusion potential within the membrane, for a membrane in contact with a 1:1 electrolyte is given by[17]:

$$\psi_m = \left(2t_g^m - 1\right)\frac{RT}{F}\ln\frac{a_s^1}{a_s^2} \tag{5}$$

where a_s^1 and a_s^2 are the activities of the salt solutions on either side of the membrane. This expression for membrane potential is derived by assuming negligible osmotic water transport across the membrane, constant ion mobilities, and small concentration differences between the two solutions.[17,29] The counter-ion transport number that appears in Equation 5 is an "apparent" transport number because it includes effects of water transport across the membrane. If water transport across the membrane is negligible, the apparent transport number and the true transport number defined by Equation 2 are essentially equal. The electric potential for an ideally selective membrane, $\psi_{m,ideal}$, is obtained when $t_g^m = 1$. The apparent membrane permselectivity is calculated from:

$$\Pi = \frac{\frac{\psi_m}{\psi_{m,ideal}} + 1 - 2t_g^s}{2t_c^s} \tag{6}$$

Often, the apparent membrane permselectivity is reported as $\psi_m/\psi_{m,ideal}$[18], though this definition is strictly valid if the transport numbers of the co-ions and counter-ions in solution are both equal to 0.5.

Ion transport in IEMs in the presence of an electric field is quantified via the membrane ionic conductivity, κ, which is given by:

$$\begin{aligned}\kappa &= -I/\frac{d\psi^m}{dx} = F^2\left(z_g^2 C_g^m u_g^m + z_c^2 C_c^m u_c^m\right)\\ &= \frac{F^2}{RT}\left(z_g^2 C_g^m D_g^m + z_c^2 C_c^m D_c^m\right)\end{aligned} \tag{7}$$

where all of the terms have been previously defined. The Einstein equation was again used to relate ionic absolute mobilities to ionic diffusivities in obtaining the expression on the right-most side. From Equation 7, ionic conductivity depends on both the counter-ion and co-ion concentrations and absolute mobilities (or diffusivities) in the membrane.

The use of membrane apparent permselectivity and ionic conductivity to illustrate a tradeoff relation in IEMs, although practically relevant for applications such as ED and RED, is not consistent with the related literature on gas separation and reverse osmosis membranes. In both of these research areas, membrane throughput is

characterized via the permeability coefficient of solute i, P_i, which is defined as the steady-state flux of i normalized by membrane thickness and driving force. The membrane selectivity, α, is defined as P_i/P_j, where i represents the more permeable species. Permeability coefficients are intrinsic membrane properties, so their use in the tradeoff relation ensures an appropriate comparison between different membranes and eliminates effects of external parameters such as thickness, different experimental conditions, etc. Herein, a new approach for illustrating the tradeoff relation in IEMs is presented. The reformulated tradeoff relation, hereafter referred to simply as the permeability-selectivity tradeoff relation, is consistent with the tradeoff relation discussed in the context of gas separation and reverse osmosis membranes. The reformulated permeability-selectivity tradeoff relation for IEMs is general and can be applied to IEMs used in different applications, as demonstrated in Section 3.4 of this report for the case of cation exchange membranes used in vanadium redox flow batteries.

3 | RESULTS AND DISCUSSION

When considering ion transport in aqueous solutions or solvent-swollen membranes, the product of ion concentrations and mobilities (or diffusivities) often appears in the mathematical description of the transport phenomena. For example, both permselectivity and ionic conductivity are related to ion concentrations and diffusivities in the membrane (see Section 2). Herein, this grouping of parameters (i.e., $z_i^2 C_i^m D_i^m$) is used to describe the permeability-selectivity tradeoff relation in IEMs. The membrane selectivity, $\alpha_{i/j}$, is defined as:

$$\alpha_{i/j} = \frac{z_i^2 C_i^m D_i^m}{z_j^2 C_j^m D_j^m} \tag{8}$$

where i is the more permeable species of the i/j pair. The parameter $\alpha_{i/j}$ is equivalent to the ratio of the total current carried by the more permeable species to the total current carried by the less permeable species. The permeability-selectivity tradeoff relation is demonstrated by plotting $\alpha_{i/j}$ versus $z_i^2 C_i^m D_i^m$.

For the case of IEMs used in ED/RED, counter-ion transport is quantified via $z_g^2 C_g^m D_g^m$ and co-ion transport is quantified via $z_c^2 C_c^m D_c^m$, so $\alpha_{g/c} = \left(z_g^2 C_g^m D_g^m\right) / \left(z_c^2 C_c^m D_c^m\right)$. Using $z_g^2 C_g^m D_g^m$ to describe counter-ion transport in IEMs instead of ionic conductivity ensures that only the transport of counter-ions within the membrane is considered. This is not the case when ionic conductivity is used for this purpose since co-ions also contribute to the membrane ionic conductivity. The reformulated permeability-selectivity tradeoff relation for IEMs used in ED/RED can be demonstrated by plotting $\alpha_{g/c}$ versus $z_g^2 C_g^m D_g^m$. Section 3.1 presents a framework for calculating $\alpha_{g/c}$ and $z_g^2 C_g^m D_g^m$ from ionic conductivity and apparent permselectivity results, which are readily available in the open literature for a broad range of materials, and Section 3.2 presents a framework for calculating $\alpha_{g/c}$ and $z_g^2 C_g^m D_g^m$ from ionic conductivity, salt permeability, and equilibrium ion sorption results. The advantages and disadvantages of both approaches are discussed.

3.1 | Calculating $\alpha_{g/c}$ and $z_g^2 C_g^m D_g^m$ from ionic conductivity and apparent permselectivity

Most studies on IEMs for ED/RED use aqueous NaCl solutions to characterize membrane properties. Thus, the following expressions are derived for an IEM in contact with an aqueous solution containing a 1:1 electrolyte (i.e., $z_g = z_c = 1$). From Equation 4, the membrane counter-ion transport number, t_g^m, is given by:

$$t_g^m = \frac{C_g^m D_g^m}{C_g^m D_g^m + C_c^m D_c^m} \tag{9}$$

Rearranging Equation 9 and inserting the definition for $\alpha_{g/c}$ yields:

$$\frac{1}{t_g^m} = \frac{C_g^m D_g^m + C_c^m D_c^m}{C_g^m D_g^m} = 1 + \frac{C_c^m D_c^m}{C_g^m D_g^m} = 1 + \frac{1}{\alpha_{g/c}} \tag{10}$$

or:

$$\alpha_{g/c} = \frac{1}{1/t_g^m - 1} = \frac{t_g^m}{1 - t_g^m} \tag{11}$$

Inserting Equation 1 into Equation 11 and rearranging yields:

$$\alpha_{g/c} = \frac{t_c^s \Pi + t_g^s}{1 - \left(t_c^s \Pi + t_g^s\right)} \tag{12}$$

Thus, $\alpha_{g/c}$ can be calculated from the experimental apparent permselectivity and the transport numbers of co-ions and counter-ions in aqueous solutions, which are tabulated in various textbooks on electrolyte solutions.[30] Combining Equations 7 and 9 yields:

$$\kappa = \frac{F^2}{RT}\left(\frac{C_g^m D_g^m}{t_g^m}\right) \tag{13}$$

Rearranging Equation 13 yields an expression for $C_g^m D_g^m$:

$$C_g^m D_g^m = \frac{\kappa t_g^m RT}{F^2} = \frac{\kappa RT\left(t_c^s \Pi + t_g^s\right)}{F^2} \tag{14}$$

Thus, $C_g^m D_g^m$ can be calculated from the experimental ionic conductivity and apparent permselectivity results and tabulated ion transport numbers in aqueous solutions.

The experimental apparent permselectivity and conductivity results presented in Figure 1 were converted to $\alpha_{g/c}$ and $C_g^m D_g^m$ using the approach outlined above. It should be noted that this approach neglects effects due to osmotic water transport across the membranes during membrane potential measurements since such effects were not accounted for in the original studies from which the results were obtained. The approach can be modified in a straightforward manner if one wishes to correct for such effects by using the expression for membrane potential that includes effects due to osmotic water transport.[17,29] Figure 2 illustrates the reformulated permeability-selectivity tradeoff plots for various CEMs and AEMs. The solid line, which represents the so-called "upper-bound", was constructed empirically to illustrate an outer boundary for the results in the open literature. The tradeoff relation between counter-ion transport ($C_g^m D_g^m$) and counter-ion/co-ion transport selectivity ($\alpha_{g/c}$) is observed in the selected data. That is, membranes that exhibit fast counter-ion transport tend to exhibit low counter-ion/co-ion selectivity and vice versa.

Several researchers have attributed this tradeoff behavior to variation in membrane water content.[18,31] Ionic conductivity of IEMs generally increases with increasing membrane water content,[32] but so does co-ion transport, which ultimately decreases apparent permselectivity. To relate the permeability-selectivity tradeoff upper bound to membrane structural parameters such as water content, theoretical models for ion concentrations and diffusivities in IEMs are needed. A predictive model for ion sorption and diffusion in homogeneous IEMs was recently reported,[33–35] and Fan and Yip have used this framework to establish a better understanding of the permselectivity-conductivity tradeoff relation in IEMs for ED/RED.[36] However, simple analytical expressions that relate the upper-bound slope and intercept to fundamental membrane properties are not available. In contrast, the basis for the permeability-selectivity tradeoff relation in gas separation membranes was elucidated by Freeman.[37] Finding a comparable theoretical explanation for the IEM tradeoff relation could help to understand the basis for the tradeoff and ultimately yield strategies to overcome it.

In general, CEMs appear to exhibit higher selectivity than AEMs for a given $C_g^m D_g^m$ value, even after accounting for inherent mobility differences between Na^+ (counter-ions in CEMs) and Cl^- (counter-ion in AEMs) ions. This observation is illustrated in Figure 3, which shows a modified tradeoff plot. To account for inherent mobility differences between Na^+ and Cl^-, membrane ion diffusion coefficients that appear in $\alpha_{g/c}$ and $C_g^m D_g^m$ were normalized by ion diffusion coefficients in solution at infinite dilution. The difference in performance between CEMs and AEMs could be due to experimental artifacts in membrane potential measurements, which were used to calculate apparent membrane permselectivity values in the original reports from which the data were extracted. Membrane potential measurements are generally performed with single or double junction reference electrodes. Not accounting for differences in the junction potentials between the reference electrodes and aqueous solutions results in artificially low apparent permselectivity values for AEMs and artificially high apparent permselectivity values for CEMs, sometimes exceeding unity.[38] Kingsbury et al. demonstrated that properly accounting for these

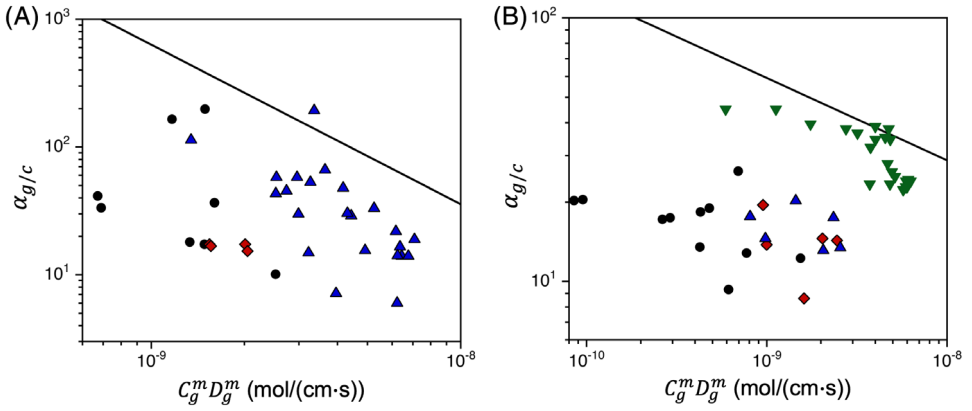

FIGURE 2 Reformulated permeability-selectivity tradeoff relation for (A) CEMs and (B) AEMs used in ED and RED. The solid line represents the empirically constructed upper-bound relation $\alpha_{g/c} = \beta / \left(C_g^m D_g^m\right)^{\lambda}$. For the CEMs, $\beta = 3.56 \times 10^{-9}$ and $\lambda = 1.25$. For the AEMs, $\beta = 9.02 \times 10^{-2}$ and $\lambda = 0.313$

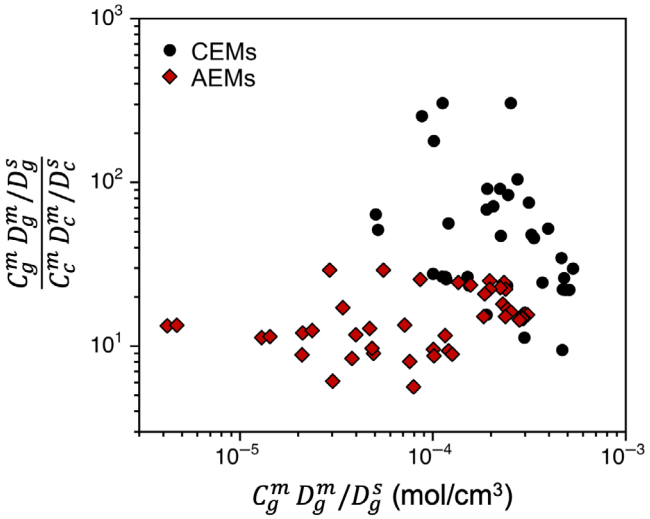

FIGURE 3 Modified permeability-selectivity tradeoff plot for IEMs. Membrane diffusion coefficients were normalized by their respective value in aqueous solution at infinite dilution (1.33×10^{-5} cm^2/s for Na^+ and 2.03×10^{-5} cm^2/s for Cl^-).[30] AEMs, anion exchange membranes; CEMs, cation exchange membranes

effects yields comparable apparent permselectivity values for commercial ion-exchange membranes CMX and AMX.[38] The results reported recently by Golubenko et al. (inverted green triangles in Figure 2(B)) for various synthesized AEMs were corrected for such effects,[22] and this is likely why the performance of these materials appears to be superior to that of the other AEMs in Figure 2(B), which were not corrected in this manner.

The observation that reference electrode junction potentials significantly influence membrane potential measurements (and therefore apparent permselectivity calculations) raises important questions about the accuracy of previously reported apparent permselectivity values that were obtained via membrane potential measurements with single or double junction reference electrodes. Recently, we demonstrated that membrane resistance measurements can be affected by interfacial resistances, which complicates the calculation of membrane ionic conductivity.[39,40] Not accounting for such effects results in artificially high membrane resistance values, particularly when dilute salt solutions are used for the measurements.[39,40] Membrane resistance measurements for the results presented in Figures 1 and 2 were performed with relatively highly concentrated NaCl solutions (0.5 M), so such effects are presumably not very significant, though likely present. Nevertheless, standardized and accurate membrane transport characterization techniques are needed to make appropriate comparisons between different IEMs and to further advance the fundamental understanding of ion transport in IEMs.

3.2 | Calculating $\alpha_{g/c}$ and $z_g^2 C_g^m D_g^m$ from ionic conductivity, salt permeability, and ion sorption

Salt permeability and equilibrium ion sorption results, which are reported less frequently than permselectivity, can also be used to calculate $\alpha_{g/c}$ and $z_g^2 C_g^m D_g^m$ when combined with ionic conductivity results. Salt permeability measurements probe concentration gradient-driven ion transport across IEMs. According to the solution-diffusion model, the salt permeability coefficient, P_s, is given by[41]:

$$P_s = K_s D_s^m = \frac{C_s^m}{C_s^s} D_s^m \tag{15}$$

where K_s is the salt sorption coefficient, D_s^m and C_s^m are the local diffusion coefficient and concentration of the mobile salt in the membrane, respectively, and C_s^s is the external solution salt concentration. For a 1:1 electrolyte, the mobile salt concentration in the membrane is equivalent to the co-ion concentration (i.e., $C_s^m = C_c^m$). The mobile salt local diffusion coefficient in the membrane, D_s^m, is related to the individual ion diffusivities and concentrations via[42]:

$$D_s^m = \frac{D_g^m D_c^m \left(C_g^m + C_c^m\right)}{C_g^m D_g^m + C_c^m D_c^m} \tag{16}$$

Counter-ion and co-ion concentrations in IEMs equilibrated with aqueous salt solutions can be determined via well-established experimental techniques.[43–45] Thus, simultaneously solving Equations 7 and 16 yields counter-ion and co-ion diffusion coefficients in IEMs.[33] Subsequently, counter-ion and co-ion concentrations and diffusion coefficients in IEMs can be used to calculate $\alpha_{g/c}$ and $C_g^m D_g^m$. The C_i^m terms that appear in Equations 7 and 16 should be based on the total membrane volume, which includes the polymer chains, water, and ions, when the experimental ion fluxes are based on the membrane geometric area.[33] This treatment is simplified if the condition $C_g^m \gg C_c^m$ is met, which is a reasonable approximation for highly charged membranes in contact with relatively dilute salt solutions.[34] If this condition is met, Equations 7 and 15 reduce to:

$$\kappa = \frac{F^2}{RT} C_g^m D_g^m \tag{17}$$

$$P_s = \frac{C_s^m}{C_s^s} D_c^m \tag{18}$$

For this limiting case, $\alpha_{g/c}$ and $C_g^m D_g^m$ can be obtained from ionic conductivity and salt permeability experiments alone.

The framework for obtaining $\alpha_{g/c}$ and $C_g^m D_g^m$ outlined in this section has several implicit assumptions. Firstly, Equation 7 for ionic conductivity assumes that the Einstein equation, which relates ionic mobilities to diffusivities, is valid for IEMs in contact with aqueous salt solutions. As mentioned previously, this assumption is strictly valid for infinitely dilute solutions, but it is a reasonable approximation for IEMs.[27] Secondly, this approach for calculating D_g^m and D_c^m assumes ion pairing in the membrane to be negligible. If mobile ions (e.g., Na^+ and Cl^-) undergo ion pairing, the ion pairs would not be detected in electric field-driven transport experiments (i.e., ionic conductivity) since they are electrically neutral, but would be detected in concentration gradient-driven transport experiments (i.e., salt permeability). For conventional IEMs, which are relatively highly charged and highly swollen, the absence of ion pairing for common electrolytes (e.g., NaCl) is a reasonable assumption.[27] Finally, apparent mobile salt diffusion coefficients obtained directly from salt permeability experiments inherently contain thermodynamic nonideal and frame of reference terms.[42] The expression given by Equation 16 is valid for mobile salt diffusion coefficients that have been corrected for such effects.

The framework for calculating $\alpha_{g/c}$ and $C_g^m D_g^m$ from ionic conductivity, salt permeability, and ion sorption results is advantageous over the framework described in Section 3.1. In the latter approach, co-ion transport is probed primarily via apparent permselectivity measurements, which are influenced by various experimental factors that can substantially affect the measurement accuracy (e.g., reference electrode junction potentials, electrolyte flow rates, osmotic water transport, etc.).[38,46] Additionally, for highly selective membranes, permselectivity values approach unity, and this causes experimental uncertainties to be magnified when calculating $\alpha_{g/c}$. For example, if we consider a CEM contacted by aqueous NaCl solutions ($t_c^s \approx 0.604$ and $t_g^s \approx 0.396$),[30] a permselectivity of 0.995 yields an $\alpha_{g/c}$ value of 330. If the experimental uncertainty for the permselectivity value is 0.002 (or 0.2%), the uncertainty in $\alpha_{g/c}$ calculated using standard propagation of uncertainty techniques is 132 (or 40% of the $\alpha_{g/c}$ value). In contrast, salt permeability coefficients can be measured quite precisely, which ultimately yields more accurate $\alpha_{g/c}$ values. Moreover, this approach for calculating $\alpha_{g/c}$ and $C_g^m D_g^m$ allows one to decouple and independently analyze the contributions from sorption and diffusion to overall membrane performance, which can yield additional insights into the fundamental transport properties.

3.3 | Influence of external solution salt concentration on $\alpha_{g/c}$ and $C_g^m D_g^m$

Equilibrium ion partitioning between IEMs and aqueous salt solutions is significantly influenced by the external solution salt concentration.[27,43,45] In general, counter-ion concentrations in IEMs are higher than those in aqueous solutions of practical interest (e.g., brackish water) due to the high concentration of fixed charge groups in IEMs. On the other hand, co-ion concentrations in IEMs are generally substantially lower than those in the external solution due to Donnan exclusion. As the salt concentration in the external solution increases, Donnan exclusion is weakened and the membrane co-ion concentration increases.[44] This increase in membrane co-ion concentration will significantly affect IEM selectivity as defined by Equation 8. To demonstrate the magnitude of this effect, Table 1 presents $C_g^m D_g^m$, $C_c^m D_c^m$, and $\alpha_{g/c}$ values for a pair of commercial IEMs as a function of external solution NaCl concentration. $C_g^m D_g^m$, $C_c^m D_c^m$, and $\alpha_{g/c}$ values were calculated from published experimental salt permeability, ionic conductivity, and ion sorption results according to the treatment outlined in 3.2.[33]

TABLE 1 $C_g^m D_g^m$, $C_c^m D_c^m$, and $\alpha_{g/c}$ values as a function of external solution NaCl concentration for commercial IEMs, CR61 and AR103

Membrane	External solution NaCl concentration (mol/L)	$C_g^m D_g^m$ [mol/(cm s)]	$C_c^m D_c^m$ [mol/(cm s)]	$\alpha_{g/c}$
CR61	1.0	3.59×10^{-9}	3.03×10^{-10}	12
	0.1	3.38×10^{-9}	9.55×10^{-12}	354
	0.01	3.40×10^{-9}	2.38×10^{-13}	14,290
AR103	1.0	2.93×10^{-9}	1.30×10^{-10}	22
	0.1	2.79×10^{-9}	3.58×10^{-12}	779
	0.01	2.72×10^{-9}	9.74×10^{-14}	27,930

From Table 1, the external solution salt concentration significantly influences membrane selectivity. For both membranes, $\alpha_{g/c}$ decreased by ~3 orders of magnitude as the external solution salt concentration increased from 0.01 to 1.0 M. This enormous change in $\alpha_{g/c}$ is almost entirely due to changes in the membrane co-ion concentration. Counter-ion and co-ion diffusivities in the membranes were nearly constant over this range of external solution salt concentration.[33] Co-ion concentrations, and therefore $C_c^m D_c^m$, increased by ~3 orders of magnitude as external solution salt concentration increased from 0.01 to 1.0 M due to weakened Donnan exclusion.[33] Counter-ion concentrations, and therefore $C_g^m D_g^m$, increased slightly with increasing external solution salt concentration due to increased co-ion sorption in the membranes and osmotic deswelling.[45] This analysis clearly demonstrates that the ability of IEMs to selectively permeate counter-ions over co-ion stems from their ability to effectively suppress co-ion sorption via Donnan exclusion.

Due to the significant effect of external solution salt concentration on IEM selectivity, it is imperative that membrane transport properties are measured at the same external solution salt concentration when comparing the performance of different IEMs.

3.4 | Permeability-selectivity tradeoff in IEMs for vanadium redox flow batteries

The reformulated permeability-selectivity tradeoff relation for IEMs is general and can be applied to essentially any application that utilizes IEMs to selectively permeate certain species. In this section, the reformulated tradeoff relation is applied to IEMs used in vanadium redox flow batteries (VRFBs). In VRFBs, IEMs are used to separate the catholyte solution, which contains the V^{5+}/V^{4+} redox couple, and the anolyte solution, which contains the V^{2+}/V^{3+} redox couple.[47,48] IEMs must allow transport of the charge balancing ions (protons for CEMs and sulfate/bisulfate for AEMs) to complete the electrical circuit and prevent crossover of the different vanadium species, which leads to self-discharge and reduced Coulombic efficiency. The past few decades have seen rapid growth in research toward developing new IEMs for VRFBs.[49–51] The majority of studies have focused on developing CEMs due to their higher ionic conductivity (lower electrical resistance) compared to AEMs, owing to the high inherent mobility of protons compared to sulfate/bisulfate. Thus, the following analysis focuses on CEMs for VRFBs.

CEM proton conductivity is generally measured via electrochemical impedance spectroscopy, and the measurements are often performed with membranes that are equilibrated in DI water.[52–56] Thus, H^+ counter-ions are the only mobile ions within the membrane, and Equation 7 reduces to:

$$\kappa = \frac{F^2}{RT} C_H^m D_H^m \tag{19}$$

where C_H^m and D_H^m are the concentration and diffusion coefficient, respectively, of H^+ ions in the membrane. Equation 19 can therefore be used to calculate $C_H^m D_H^m$ from ionic conductivity measurements performed on membranes equilibrated with DI water. The $C_H^m D_H^m$ values calculated from ionic conductivity measurements on IEMs equilibrated with DI water are idealized and not representative of an operating VRFB since vanadium species are not present during the measurements. Ionic conductivity measurements are sometimes performed with membranes equilibrated with sulfuric acid solutions[57–59] or a mixture of sulfuric acid and vanadyl sulfate,[60] though these experimental conditions are less common. In this case, the full expression for ionic conductivity (Equation 7) describes electric field driven transport across the membrane.

Vanadium transport across IEMs for VRFBs is often probed using vanadium permeability experiments. These experiments are performed with standard diffusion cells, in which the upstream chamber contains highly concentrated solutions of $VOSO_4$ (typically between 1 and 1.5 M) and H_2SO_4 (typically between 2 and 3 M), and the downstream chamber contains $MgSO_4$ and H_2SO_4 at concentrations equivalent to those of $VOSO_4$ and H_2SO_4, respectively, in the upstream chamber.[52–66] The change in vanadium concentration in the downstream chamber is tracked as a function of time, and the vanadium permeability coefficient is calculated from the pseudo steady-state vanadium flux across the membrane, the vanadium concentration difference across the membrane, and the membrane thickness. Equation 18 can be used to relate the vanadium permeability coefficient, P_V, to the vanadium concentration (C_V^m) and diffusion coefficient (D_V^m) in the membrane:

$$C_V^m D_V^m = P_V C_V^s \tag{20}$$

where C_V^s is the vanadium concentration of the upstream solution. It should be noted that the vanadium permeability experiments discussed in this section are different from the salt permeability experiments discussed in Section 3.2. In the salt permeability experiments, salt molecules (i.e., sodium and chloride ions) diffuse as a pair across the membrane from the high concentration side to the low concentration side, whereas in the vanadium

permeability experiments, vanadium diffusion is counterbalanced by magnesium diffusion in the opposite direction. Thus, this experimental setup is not rigorously representative of an operating VRFB, and vanadium permeability coefficients may be influenced by magnesium counter diffusion.

In most studies on IEMs for VRFBs, selectivity is expressed as the ratio of ionic conductivity to vanadium permeability (i.e., κ/P_V).[67] Within the framework developed in the present study, the selectivity of CEMs used in VRFBs, $\alpha_{H/V}$, is obtained via:

$$\alpha_{H/V} = \frac{C_H^m D_H^m}{4C_V^m D_V^m} = \frac{\kappa RT}{4F^2 P_V C_V^s} \tag{21}$$

The factor of four in the denominator of Equation 21 comes from the valence of VO^{2+}.

Proton conductivity and vanadium permeability results from the open literature were used to calculate $C_H^m D_H^m$ and $\alpha_{H/V}$ for various CEMs according to the approach described above. Figure 4 presents a summary of the results in the format of a permeability-selectivity tradeoff plot. The data used to generate the plot in Figure 4 are recorded in Data S2. In these studies, the $VOSO_4$ concentration used for the vanadium permeability experiments varied from 1 to 1.5 M, and the sulfuric acid concentration varied from 2 to 3 M. The concentration dependence of vanadium permeability coefficients has not been studied for a broad range of materials, but there is evidence that vanadium permeability coefficients do not change significantly with vanadium concentration when the sulfuric acid concentration is greater than 2 M.[66] Thus, plotting all of these results on the same permeability-selectivity tradeoff plot, though not entirely rigorous, appears to be reasonable. A tradeoff between $C_H^m D_H^m$ and $\alpha_{H/V}$ for CEMs used in VRFBs is observed in Figure 4. That is, membranes that exhibit fast proton transport generally have low proton/vanadium selectivity and vice versa. A fundamental basis for the permeability-selectivity tradeoff relation in IEMs for VRFBs is not available as there are currently no fundamental models that can accurately predict partitioning and diffusion of mixed electrolytes in IEMs. Better fundamental understanding of ion partitioning and diffusion in IEMs for VRFBs could enable rational design of high-performance membranes that overcome this tradeoff.

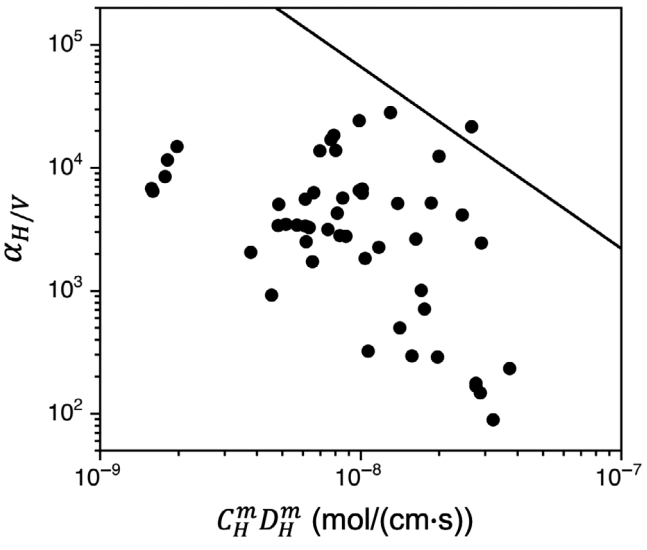

FIGURE 4 Reformulated permeability-selectivity tradeoff relation for IEMs used in VRFBs. The solid line represents the empirically constructed upper-bound relation $\alpha_{H/V} = \beta/\left(C_H^m D_H^m\right)^{\lambda}$, where $\beta = 2.82 \times 10^{-9}$ and $\lambda = 1.65$

4 | CONCLUSIONS

The permselectivity-conductivity tradeoff relation for IEMs was reformulated in terms of ion concentrations and diffusion coefficients in the membrane. The reformulated tradeoff relation is generalizable to applications other than ED/RED and is more consistent with the related literature on the permeability-selectivity tradeoff relations for gas separation and reverse osmosis membranes. A framework for extracting the counter-ion/co-ion selectivity, $\alpha_{g/c}$, and counter-ion transport, $C_g^m D_g^m$, from membrane permselectivity and ionic conductivity results was presented. In general, $\alpha_{g/c}$ decreased with increasing $C_g^m D_g^m$, demonstrating the tradeoff between counter-ion transport and counter-ion/co-ion selectivity for IEMs used in ED/RED applications. For a given $C_g^m D_g^m$ value, CEMs generally exhibited higher $\alpha_{g/c}$ relative to AEMs, though this may be due to experimental issues associated with membrane potential measurements rather than differences in intrinsic membrane properties. A framework for extracting the parameters $\alpha_{g/c}$ and $C_g^m D_g^m$ from salt permeability, ionic conductivity, and equilibrium ion sorption results was also presented. This framework is advantageous over the framework based on membrane permselectivity due to the more precise measurement of co-ion transport across membranes. The generalizability of the reformulated tradeoff relation was demonstrated by extending the analysis to CEMs used in VRFBs. A tradeoff between proton transport and proton/vanadium selectivity was observed, whereby membranes that exhibited fast proton transport exhibited low proton/vanadium selectivity and vice versa. The reformulated permeability-selectivity tradeoff relation presented herein allows clear evaluation of IEM performance for essentially any application that uses IEMs.

ACKNOWLEDGMENTS

The author would like to thank David Kitto, José C. Díaz, Carolina Espinoza, and Cassidy Carey for fruitful discussions and for proofreading the manuscript.

CONFLICT OF INTEREST

The authors declare no competing financial interest.

ORCID

Jovan Kamcev https://orcid.org/0000-0003-0379-5171

REFERENCES

[1] T. Xu, C. Huang, *AIChE J.* **2008**, *54*, 3147.
[2] M. Y. Kariduraganavar, R. K. Nagarale, A. A. Kittur, S. S. Kulkarni, *Desalination* **2006**, *197*, 225.
[3] H. Jaroszek, P. Dydo, *Open Chem.* **2016**, *14*, 1.
[4] H. Strathmann, A. Grabowski, G. Eigenberger, *Ind. Eng. Chem. Res.* **2013**, *52*, 10364.
[5] J. Luo, C. Wu, T. Xu, Y. Wu, *J. Membr. Sci.* **2011**, *366*, 1.
[6] J. Jang, Y. Kang, J.-H. Han, K. Jang, C.-M. Kim, I. S. Kim, *Desalination* **2020**, *491*, 114540.
[7] E. Güler, R. Elizen, D. A. Vermaas, M. Saakes, K. Nijmeijer, *J. Membr. Sci.* **2013**, *446*, 266.
[8] K.-D. Kreuer, *Chem. Mater.* **2014**, *26*, 361.
[9] G. Merle, M. Wessling, K. Nijmeijer, *J. Membr. Sci.* **2011**, *377*, 1.
[10] L. Zeng, T. S. Zhao, L. Wei, H. R. Jiang, M. C. Wu, *Appl. Energy* **2019**, *233–234*, 622.
[11] C. A. Machado, G. O. Brown, R. Yang, T. E. Hopkins, J. G. Pribyl, T. H. Epps, *ACS Energy Lett.* **2020**, *15*, 158.
[12] S. Das, K. Dutta, D. Rana, *Polym. Rev.* **2018**, *58*, 610.
[13] A. Oehmen, R. Viegas, S. Velizarov, M. A. M. Reis, J. G. Crespo, *Desalination* **2006**, *199*, 405.
[14] D. M. Weekes, D. A. Salvatore, A. Reyes, A. Huang, C. P. Berlinguette, *Acc. Chem. Res.* **2018**, *51*, 910.
[15] M. R. Singh, E. L. Clark, A. T. Bell, *Phys. Chem. Chem. Phys.* **2015**, *17*, 18924.
[16] Y. Tanaka, *Ion Exchange Membrane Electrodialysis: Fundamentals*, Desalination, Separation, Nova Science Publishers, New York **2010**.
[17] H. Strathmann, *Ion-Exchange Membrane Separation Processes*, Elsevier, Amsterdam **2004**.
[18] G. M. Geise, M. A. Hickner, B. E. Logan, *ACS Appl. Mater. Interfaces* **2013**, *5*, 10294.
[19] H. B. Park, J. Kamcev, L. M. Robeson, M. Elimelech, B. D. Freeman, *Science* **2017**, *356*, eaab0530.
[20] H. Fan, Y. Huang, N. Y. Yip, *J. Membr. Sci.* **2020**, *610*, 118259.
[21] D. V. Golubenko, G. Pourcelly, A. B. Yaroslavtsev, *Sep. Purif. Technol.* **2018**, *207*, 329.
[22] D. V. Golubenko, B. Van der Bruggen, A. B. Yaroslavtsev, *J. Appl. Polym. Sci.* **2020**, *137*, 48656.
[23] I. Stenina, D. Golubenko, V. Nikonenko, A. Yaroslavtsev, *Int. J. Mol. Sci.* **2020**, *21*, 5517.
[24] K. H. Lee, D. H. Cho, Y. M. Kim, S. J. Moon, J. F. Kim, Y. M. Lee, *J. Membr. Sci.* **2017**, *535*, 35.
[25] D. H. Cho, K. H. Lee, Y. M. Kim, S. H. Park, W. H. Lee, S. M. Lee, Y. M. Lee, *Chem. Commun.* **2017**, *53*, 2323.
[26] L. Cseri, J. Baugh, A. Alabi, A. AlHajaj, L. Zou, R. A. W. Dryfe, P. M. Budd, G. Szekely, *J. Mater. Chem. A* **2018**, *6*, 24728.
[27] F. Helfferich, *Ion Exchange*, Dover Publications, New York, reprint **1995**.
[28] Y. Tanaka, *Ion Exchange Membranes: Fundamentals and Applications*, 2nd ed., Oxford: Elsevier Inc, **2015**.
[29] N. Lakshminarayanaiah, *Transport Phenomena in Membranes*, Academic Press, New York **1972**.
[30] R. A. Robinson, R. H. Stokes, *Electrolyte Solutions*, Dover Publications, Mineola, NY **2002**.
[31] S. T. Russell, R. Pereira, J. T. Vardner, G. N. Jones, C. Dimarco, A. C. West, S. K. Kumar, *Macromolecules* **2020**, *53*, 1014.
[32] E. P. Chan, B. R. Frieberg, K. Ito, J. Tarver, M. Tyagi, W. Zhang, E. B. Coughlin, C. M. Stafford, A. Roy, S. Rosenberg, C. L. Soles, *Macromolecules* **2020**, *53*, 1443.
[33] J. Kamcev, D. R. Paul, G. S. Manning, B. D. Freeman, *Macromolecules* **2018**, *51*, 5519.
[34] J. Kamcev, D. R. Paul, G. S. Manning, B. D. Freeman, *ACS Appl. Mater. Interfaces* **2017**, *9*, 4044.
[35] J. Kamcev, M. Galizia, F. M. Benedetti, E. S. Jang, D. R. Paul, B. D. Freeman, G. S. Manning, *Phys. Chem. Chem. Phys.* **2016**, *18*, 6021.
[36] H. Fan, N. Y. Yip, *J. Membr. Sci.* **2019**, *573*, 668.
[37] B. D. Freeman, *Macromolecules* **1999**, *32*, 375.
[38] R. S. Kingsbury, S. Flotron, S. Zhu, D. F. Call, O. Coronell, *Environ. Sci. Technol.* **2018**, *52*, 4929.
[39] J. Kamcev, R. Sujanani, E.-S. Jang, N. Yan, N. Moe, D. R. Paul, B. D. Freeman, *J. Membr. Sci.* **2018**, *547*, 123.
[40] J. C. Díaz, J. Kamcev, *J. Membr. Sci.* **2021**, *618*, 118718.
[41] G. M. Geise, D. R. Paul, B. D. Freeman, *Prog. Polym. Sci.* **2014**, *39*, 1.
[42] J. Kamcev, D. R. Paul, G. S. Manning, B. D. Freeman, *J. Membr. Sci.* **2017**, *537*, 396.
[43] G. M. Geise, L. P. Falcon, B. D. Freeman, D. R. Paul, *J. Membr. Sci.* **2012**, *423–424*, 195.
[44] J. Kamcev, D. R. Paul, B. D. Freeman, *J. Mater. Chem. A* **2017**, *5*, 4638.
[45] J. Kamcev, D. R. Paul, B. D. Freeman, *Macromolecules* **2015**, *48*, 8011.
[46] Y. Ji, G. M. Geise, *Ind. Eng. Chem. Res.* **2017**, *56*, 7559.
[47] P. Alotto, M. Guarnieri, F. Moro, *Renew. Sustain. Energy Rev.* **2014**, *29*, 325.
[48] Á. Cunha, J. Martins, N. Rodrigues, F. P. Brito, *Int. J. Energy Res.* **2015**, *39*, 889.
[49] S. Maurya, S. H. Shin, Y. Kim, S. H. Moon, *RSC Adv.* **2015**, *5*, 37206.
[50] B. Schwenzer, J. Zhang, S. Kim, L. Li, J. Liu, Z. Yang, *ChemSusChem* **2011**, *4*, 1388.
[51] H. Prifti, A. Parasuraman, S. Winardi, T. M. Lim, M. Skyllas-Kazacos, *Membranes* **2012**, *2*, 275.
[52] T. Wang, S. J. Moon, D. S. Hwang, H. Park, J. Lee, S. Kim, Y. M. Lee, S. Kim, *J. Membr. Sci.* **2019**, *583*, 16.
[53] X. B. Yang, L. Zhao, X. L. Sui, L. H. Meng, Z. B. Wang, *J. Colloid Interface Sci.* **2019**, *542*, 177.
[54] H. Y. Jung, M. S. Cho, T. Sadhasivam, J. Y. Kim, S. H. Roh, Y. Kwon, *Solid State Ionics* **2018**, *324*, 69.
[55] L. Semiz, N. Demirci Sankir, M. J. Sankir, *Membr. Sci.* **2014**, *468*, 209.

[56] Y. Zhang, J. Li, L. Wang, S. J. Zhang, *Solid State Electrochem.* **2014**, *18*, 3479.
[57] X. Yan, C. Zhang, Z. Dong, B. Jiang, Y. Dai, X. Wu, G. He, *ACS Appl. Mater. Interfaces* **2018**, *10*, 32247.
[58] S. W. Choi, T. H. Kim, S. W. Jo, J. Y. Lee, S. H. Cha, Y. T. Hong, *Electrochim. Acta* **2018**, *259*, 427.
[59] H. Zhang, H. Zhang, X. Li, Z. Mai, W. Wei, Y. Li, *J. Power Sources* **2012**, *217*, 309.
[60] X. Song, L. Ding, L. Wang, M. He, X. Han, *Electrochim. Acta* **2019**, *295*, 1034.
[61] J. Ye, Y. Cheng, L. Sun, M. Ding, C. Wu, D. Yuan, X. Zhao, C. Xiang, C. Jia, *J. Membr. Sci.* **2019**, *572*, 110.
[62] J. Zhou, Y. Liu, P. Zuo, Y. Li, Y. Dong, L. Wu, Z. Yang, T. Xu, *J. Membr. Sci.* **2020**, *620*, 118832.
[63] D. G. Oei, *J. Appl. Electrochem.* **1985**, *15*, 231.
[64] W. Xie, R. M. Darling, M. L. Perry, *J. Electrochem. Soc.* **2016**, *163*, A5084.
[65] D. Chen, M. A. Hickner, E. Agar, E. C. Kumbur, *Electrochem. Commun.* **2013**, *26*, 37.
[66] J. S. Lawton, A. Jones, T. Zawodzinski, *J. Electrochem. Soc.* **2013**, *160*, A697.
[67] S. Jiang, S. Lu, Y. Xiang, S. P. Jiang, *Adv. Sustain. Syst.* **2019**, *3*, 1900020.

SUPPORTING INFORMATION

Additional supporting information may be found online in the Supporting Information section at the end of this article.

How to cite this article: J. Kamcev, *J Polym Sci* **2021**, *59*(21), 2510. https://doi.org/10.1002/pol.20210304